HARMONIC ANALYSIS AND MODELING OF TRANSFORMERLESS ELECTRIC RAILWAY TRACTION DRIVES

Farhad Shahnia[1], Mohammad B.B. Sharifian[2]
[1] East Azarbayjan Electric Power Distribution Company, Tabriz, Iran
[2] Faculty of Electrical and Computer Engineering, University of Tabriz, Tabriz, Iran
farhadshahnia@yahoo.com, sharifian@tabrizu.ac.ir

Abstract. The design of the electrical distribution system of electrified railways includes single-phase 1x25 or two-phase 2x25 kV AC systems. Most of the electric railways use AC induction motors as their electric drives for their better characteristics and costs in comparison with other kinds of motors. Previously, a transformer was utilized in the electric train for reducing the catenary voltage to the rated voltage of the induction motor. A transformerless connection for feeding the induction motor is presented in this paper. This structure is used for converting single phase AC voltage of the catenary to DC and converting the DC voltage to three phase AC voltage with a PWM controlled inverter. In such a structure, harmonic currents injected into the power system during the PWM switching process are low. Through the whole paper, current harmonics are measured analytically and also modelled with PSCAD/EMTDC software. The results of the simulation include the waveforms of the system current and the magnitude of THD. Using such a structure can reduce the necessity of using a transformer for feeding the induction motor and also reduce the amounts of harmonics injected to the power system greatly.

Keywords. Electrified railway, Induction motor, Transformerless connection, Harmonic analysis

1. INTRODUCTION

With utilization of voltage source inverters, AC traction motors are presently common in electric railway traction applications. Several AC motors such as switched reluctance, permanent magnet synchronous and asynchronous motors are being used widely in electrified traction applications. Meanwhile, induction motors are being used as the most popular AC motors for the electrified traction systems. Every electric railway car manufacturing company uses one of the mentioned motor structures for traction force generation which is needed to run the train sets.

Several European railway networks supply their rolling stock from single phase 15 or 25 kV with 60, 50, or $16^{2/3}$ Hz frequencies. Therefore, the railway vehicles are equipped with a transformer to reduce the line voltage to a more convenient level for the motor and semiconductors. At such variable frequencies, the medium voltage transformer suffers from poor efficiency and high weight. Several research activities have been going on to substitute the transformer by power electronic concepts to improve it by superconductors. Considering the power electronic alternatives, different solutions are proposed either with an intermediate conversion stage using medium frequency transformers or transformerless configuration [1].

Usually, there are four induction motors on each of cars of a train set used for generating the sufficient traction force for the train sets. The induction motors are fed through inverters which supply the 0.4 kV, 3 ph, 50 Hz power demand of the induction motors. The connections of the induction motors can be changed from series to parallel modes which enables higher electric torque at starting and braking times for achieving the required acceleration and deceleration ratings by connecting them in series and having higher speed at normal conditions by connecting them in parallel. The schematic diagram of the drive system of induction motors on every car is shown in Fig. 1.

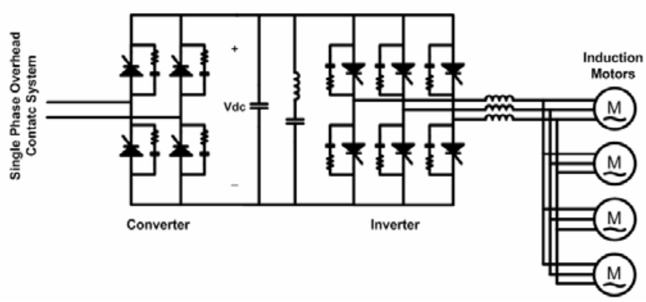

Fig. 1. Schematic diagram of the drive system of induction motors on every car of the train sets

In this paper, the converter design of an induction motor with transformerless approach is studied for traction applications. This system consists of a cascaded converter and inverter which are serving different jobs such as producing three-phase, 50 Hz, 0.4 kV output voltage for the induction motors through the input voltage with any amplitude and frequency. This structure is used for converting single phase AC voltage of the catenary to DC and converting the DC voltage to three phase AC voltage with a PWM controlled inverter. In such a structure, harmonic currents injected into the power system during the PWM switching process are low. Through the whole paper, current harmonics are studied analytically. The simulation is done with PSCAD/EMTDC software where the results of the simulation include the waveforms of the system current and the magnitude of THD. Using such a structure can reduce the necessity of using a transformer for feeding the induction motor and also reduce the amounts of harmonics injected to the power system greatly.

2. DYNAMIC CHARACTERISTICS OF INDUCTION MOTOR FOR TRACTION APPLICATIONS

Traction loads require a high torque at starting to meet the train resistance and acceleration effort. Also because of the irregular interruptions on the pantograph structure of the trains, the interruptions should not cause distress to the traction motor by way of current rush and its associated ill-effects. The induction motor should also be capable of dynamic regenerative braking which enables the possibility of running the motor as generator that can impart considerable advantages to electric traction by way of saving the regenerated power in most situations.

The development of power electronics such as GTO or IGBT has led to application of induction motors for traction purposes through invention and accurate control of PWM controlled variable voltage variable frequency (VVVF) inverters which give a VVVF output from a DC input. Therefore, the need for an in-built series characteristic for self-regulation becomes redundant if an induction motor is fed with VVVF supply because it eliminates the main draw backs of an induction motor such as switchings in speed and torque control methods [2].

For studying the power consumption of the induction motors, it is necessary to investigate the dynamical behaviour of the traction system loads along the route such as the starting and stopping times and the curvature and gradient of the route. Fig. 2 shows the typical speed profile of a train set between two stations. When the train starts from the station, it operates in constant acceleration mode as shown in region I. As the speed reaches 22 km/hour, the operation mode is changed to constant power in region II. When the speed is above 37 km/hour, the train set is operated in constant slip mode where the traction effort is inversely proportional to the square of the train speed, as shown in region III. After the speed reaches the cruising speed, the train operates with coasting mode without applying any input propulsion power, shown in region IV. When the train approaches the next station, the electric regeneration braking is applied by operating the induction motors as induction generators so that the kinetic energy of the train set can be converted into electricity to achieve the energy conservation as shown in region V. For each operation mode, the power demand of the train set can be solved based on the acceleration and various types of train resistance. Therefore, the power demand of a train set from the first station to the last one along the route resembles Fig. 3.

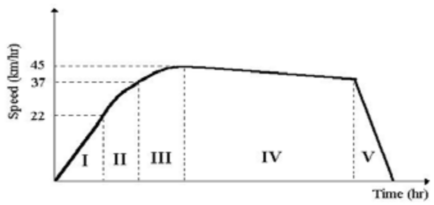

Fig. 2. Speed characteristics of the train sets with time and place variation

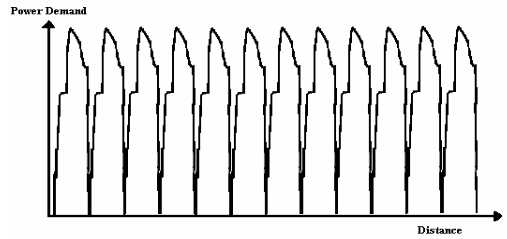

Fig. 3. Power demand characteristic of a train set from the first station to the last one, along the route

3. HARMONIC ANALYTICAL STUDIES

The circuit of a PWM controlled converter, sometimes refereed as a four quadrant controller was shown in Fig. 1. The circuit configuration consists of a conventional bridge rectifier with the addition of active switching device. The circuit can operate in all the four quadrants of the input voltage-current plane and features near unity power factor operation, easy transition from motoring to regenerative braking and draws near sinusoidal line current by the PWM control method [3,4].

One of the main aspects in the design of the PWM controlled converter is the PWM scheme. Since the harmonics generated by the PWM converter during the processes affects the performance and manufacturing costs of the whole drive system, it is necessary to study the behavior of the equipment in the operation time. A computer simulation, in addition to a theoretical solution, is necessary to reveal the mechanism of the harmonic generation and cancellation. Several PWM schemes can be used which have different effects on the current harmonic spectrum. In this paper, the 2-dimentional and 3-dimensional models of a PWM controlled inverter are studied and used for deriving the formulas of the harmonic spectrum of the PWM converters [5,7].

Fig. 4 illustrates the generation of the double edge modulated pulse train of a PWM converter bridge. Fig. 2a is the 2-D model showing the method of generating the pulse train. Fig. 2b is the 3-D model used for analyzing the pulse train frequency spectrum. Combining the 2-D and 3-D models help us in studying the harmonic generation mechanism, visually. For the 2-D model as shown in Fig. 2a the two modulation waveforms +V, and –V, are compared with the carrier waveform. The carrier changes slope every half carrier cycle. Both the modulation waveform and the carrier extend along the time axis.

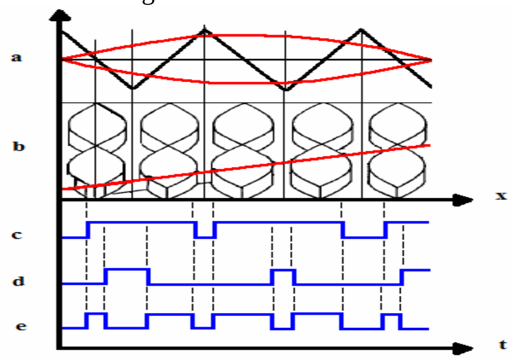

Fig. 4. 2-D and 3-D representations of a PWM controlled converter

In the 3-D model, the intersection wall follows the ratio of $M_R=\omega_c/\omega_m$ with no change in the slope, while the modulation waveform and intersection extends along the x and y axes. Imagine a wall parallel with the x axis and cutting through the walls formed by the modulation waveforms. This will result in a pulse train which is repetitive along the x axis every M_R carrier period and along the y axis every modulation period. The pulse train generated by the intersection wall with the modulation waveforms arranged will contain modulation information along both the x and y axes, as shown in Fig. 2b.

A pulse train resulting from any PWM modulation similar to Fig. 2b can be expressed by:

$$F(x,y)=\frac{1}{2}A_0+\sum_{n=1}^{\infty}\left[A_n\cos(ny)+B_n\sin(ny)\right]+\sum_{m=1}^{\infty}\left[A_m\cos(my)+B_m\sin(my)\right]+\sum_{m=1}^{\infty}\sum_{n=\pm 1}^{\pm\infty}\left[A_{mn}\cos(mx+ny)+B_{mn}\sin(mx+ny)\right] \quad (1)$$

where

$$A_{mn}=\frac{1}{2\pi^2}\int_0^{2\pi}\int_0^{2\pi}F(x,y).\cos(mx+ny)dx.dy$$
$$B_{mn}=\frac{1}{2\pi^2}\int_0^{2\pi}\int_0^{2\pi}F(x,y).\sin(mx+ny)dx.dy \quad (2)$$

where, the first term is the DC component of the pulse; the second term is the frequency component of the modulating waveform and its harmonics; the third term is the carrier waveform frequency component and the last term is the crossmodulation components of the carrier and the modulating waveforms. The final result of the spectrum is obtained by replacing x and y in fourier series by the time functions of $\omega_c.t$ *and* $\omega_m.t$, respectively. The double Fourier series method is now applied to the PWM converter. It is proved that the harmonic spectrum of $V_c(t)$ contains two main parts. The modulation waveform frequency component as:

$$\sum_{n=1,3,5,\ldots}^{\infty}\frac{4J_n\left(n\varepsilon p\frac{M_I\pi}{2}\right)}{n\varepsilon p\pi}.\sin\left(n\omega_m t-\frac{n\varepsilon p\pi}{2}\right) \quad (3)$$

and the crossmodulation components as:

$$\sum_{n=2,4,6,\ldots}^{\infty}\sum_{n=1,3,5,\ldots}^{\infty}4.C_{mn}(-1)^{\frac{m}{2}}\times\sin\left[\left(m\omega_c t+n\omega_m t\right)-\left(m\pi+\frac{n\varepsilon p\pi}{2}\right)\right] \quad (4)$$

4. SIMULATION RESULTS

In this paper, the transformerless connection of the electrical machine drive for an AC electrified railway system is simulated with PSCAD/EMTDC software. The converter and inverter structure and configuration as shown in Fig. 1 are PWM controlled, feeding the induction motors in the purpose of eliminating the transformer. The DC voltage is feeding the voltage source inverter through a LC filter. The capacitor of this filter is used for reducing the ripples of the DC voltage caused by the converters in the traction substations and the reactance for reducing the ripples of the current passing through the inverter. The three phase output of the inverter again passes through low value reactances for minimizing the THD of the AC current feeding the induction motors. The three phase AC voltage at the output side of the inverter is shown in Fig. 5 with the RMS value as shown in Fig. 6.

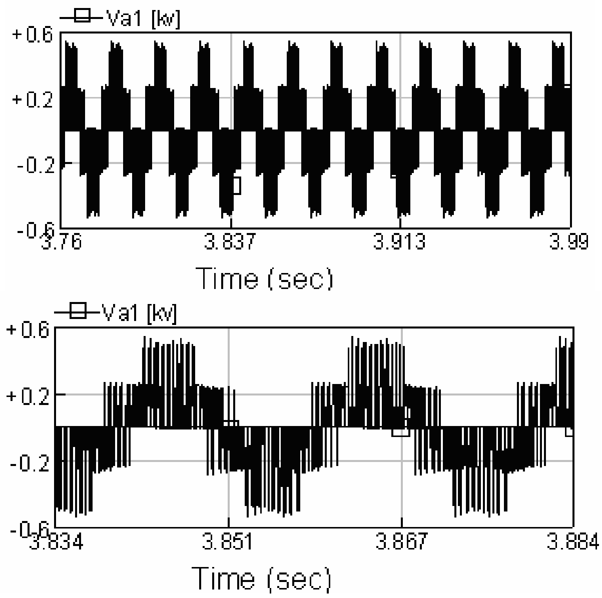

Fig. 5. The output voltage of the PWM controlled inverter feeding the induction motors

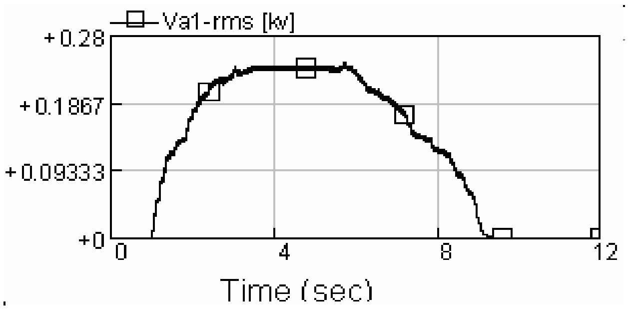

Fig. 6. RMS waveform of the output voltage of the PWM controlled inverter feeding the induction motors

The DC current feeding the VSI of the induction motors in the traction system for the simulated study case is shown in Fig. 7. It is shown that during the accelerating time, the amplitude of the current increases, it is almost constant in the constant speed mode and it will decrease and flow back from the inverter to the DC bus, during regenerating braking mode. If the conventional braking is happened instead of the regenerative, the current values decreases to constant value of zero.

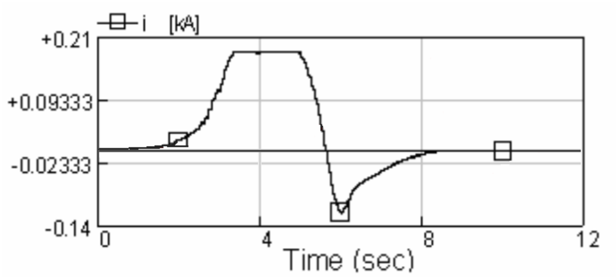

Fig. 7. The feeding DC current of the inverters for the simulated study case

The RMS output current of the inverter is also shown in Fig. 8. It can be understood that at the accelerating time, the current increases but it reaches to its steady state value very fast and when regenerative braking happens, there is an overshoot in the decreasing waveform of the current because of the reactive part of the current because the induction machine consumes reactive power in generator mode. Providing conventional braking instead of regenerative, the current waveform would decrease to constant value of zero without a sudden overshoot.

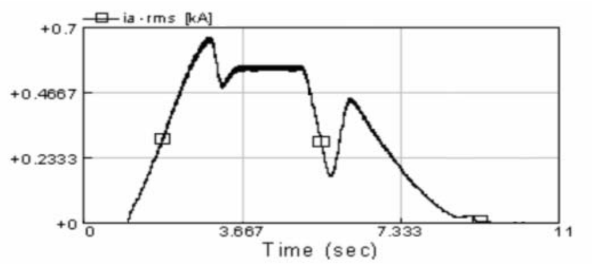

Fig. 8. RMS output current of the inverters of the simulated study case

The active and reactive power waveforms of the simulated traction drive set are shown in Fig. 9. The regenerated current waveform going back from the induction motors to the overhead catenary line is shown in Fig. 10.

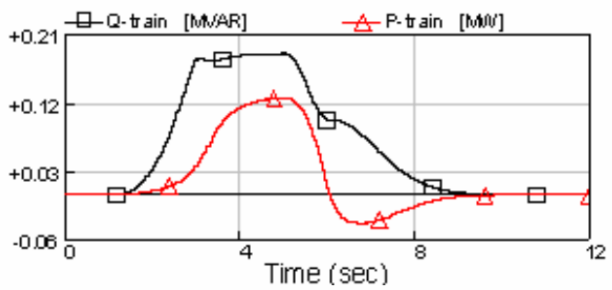

Fig. 9. Active and reactive power consumption of the induction motors on the simulated traction system

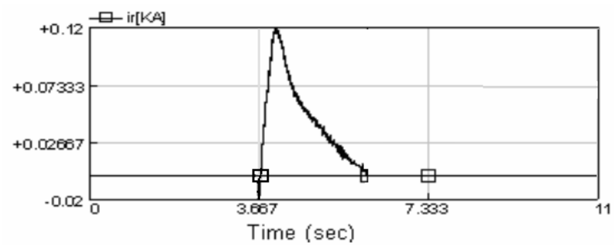

Fig. 10. DC current in the resistor bank in the traction substation

The electrical and mechanical torques of the induction motor fed through the transformerless configuration is shown in Figures 13 and 14, respectively. Because of the losses, the values of the mechanical torque are a little bit smaller than the electrical torque values.

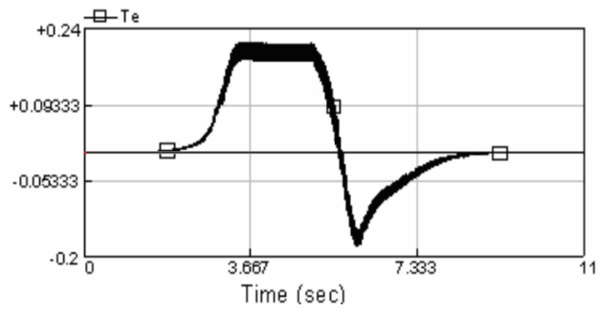

Fig. 11. Electrical torque of the simulated induction motor for traction application

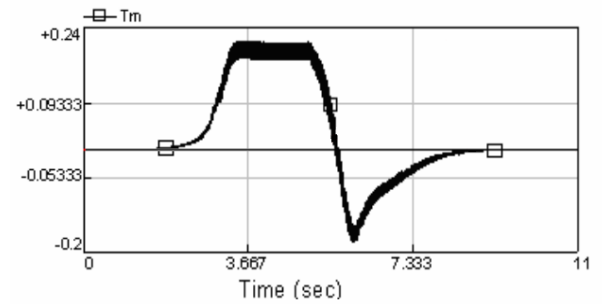

Fig. 12. Mechanical torque of the simulated induction motor for traction application

5. CONCLUSION

The design of the electrical distribution system of electrified railways includes single-phase 1x25 or two-phase 2x25 kV AC systems with 60, 50 or $16^{2/3}$ Hz frequencies. There is usually a transformer in the train for reducing the catenary voltage to the rated voltage feeding the inverter fed induction motors. In this paper, a transformerless connection for feeding the induction motor is presented by utilizing a converter for converting single phase AC voltage of the catenary to DC and a PWM controlled inverter for transforming the DC voltage to three phase AC voltage. Through the whole paper, the current harmonics injected into the power system during the PWM switching process were studied analytically and through the simulation results with PSCAD/EMTDC software. Using such a structure can reduce the necessity of using a transformer for feeding the induction motor and also reduce the amounts of harmonics injected to the power system greatly.

6. REFERENCES

[1] Dieckerhoff S., Bemet S., Krug D., "Evaluation of IGBT multilevel converters for transformerless traction applications", IEEE 34^{th} Annual Power Electronics Specialist Conf., Vol. 4, 2003, pp. 1757-1763.

[2] Shen J., Butterworth N., “Analysis and design of a three-level PWM converter system for railway-traction applications”, Proc. of Inst. Elect. Eng., Elect. Power Applications, Vol. 144, 1997, No. 5, pp. 357–371.
[3] Lordache M., Mendes E., Marchand C., Belin S., Mickiewicz V., "Harmonic analysis method for traction drives EMI studies", IEE Proc. of Electr. Power Applications, Vol. 150, 2003, No. 4, pp. 431-438.
[4] Holmes D.G., “A general analytical method for determining the theoretical harmonic components of carrier based PWM strategies”, Proc. of 33rd Industrial Applications Society Annual Meeting, Vol. 2, 1998, pp. 1207–1214.
[5] Shen J., Taufig J.A., and Mansell A.D., “Analytical solution to harmonic characteristics of traction PWM converters”, Proc. of Inst. Elect. Eng., Elect. Power Applications, Vol. 144, 1997, No. 2, pp. 158–168.
[6] Shen J., Taufiq J.A., Mansell A.D., "Analytical solution to harmonic characteristics of traction PWM converters", IEE Proc. on Electrical Power Applications, Vol. 144, 1997, No. 2.
[7] Chang G.W., Lin H.W., Chen S.K., "Modelling Characteristics of Harmonic Currents Generated by High Speed Railway Traction Drive Converters", IEEE Trans. on Power Delivery, Vol. 19, 2004, No. 2, pp. 766-773.